Title: Autocrine Adenosine Regulates Tumor Polyfunctional CD73lt;supgt;+lt;/supgt;CD4lt;supgt;+lt;/supgt; Effector T Cells Devoid of Immune Checkpoints.

Authors: Gourdin N, Bossennec M, Rodriguez C, Vigano S, Machon C, Jandus C, Bauché D, Faget J, Durand I, Chopin N, Tredan O, Marie JC, Dubois B, Guitton J, Romero P, Caux C, Ménétrier-Caux C

Journal: Cancer research

Year: 2018 Jul 1

Issue: 78

Volume: 13

Pages: 3604-3618

DOI: 10.1158/0008-5472.CAN-17-2405

Title : Autocrine Adenosine regulates tumor polyfunctional $CD73^+CD4^+$ effector T cells devoid of immune checkpoints

Nicolas Gourdin[1,2,3,] Marion Bossennec[1,2], Céline Rodriguez[1,2,3], Selena Vigano[4], Christelle Machon[5,6], Camilla Jandus[4], David Bauché[2,8,10], Julien Faget[1,2,3], Isabelle Durand[2,9], Nicolas Chopin[11], Olivier Tredan[11], Julien C. Marie[2,8,10], Bertrand Dubois[1,2], Jérôme Guitton[5,7], Pedro Romero[4], Christophe Caux[1,2,3†], Christine Ménétrier-Caux[1,2,3†*]. ([†]: Co-last authorship)

Affiliations:
[1] Team 11, INSERM U1052, Cancer Research Center of Lyon, F-69008 Lyon, France
[2] Univ Lyon, Université Claude Bernard Lyon 1, INSERM 1052, CNRS 5286, Centre Léon Bérard, Centre de recherche en cancérologie de Lyon, Lyon, 69008, France
[3] Innovation and translational research department of Department, Centre Léon Bérard, Lyon, F-69008, France
[4]Ludwig Cancer Research Center, Department of Oncology, Faculty of Biology and Medicine, University of Lausanne, Lausanne, Switzerland
[5]Hospices Civils de Lyon, Centre Hospitalier Lyon-Sud, Laboratoire de Biochimie et Toxicologie, F-69495 Pierre-Bénite, France
[6]Université de Lyon, Université Lyon 1, ISPB Faculté de pharmacie, Laboratoire de Chimie Analytique, F-69008 Lyon, France
[7]Université de Lyon, Université Lyon 1, ISPB Faculté de pharmacie, Laboratoire de Toxicologie, F-69008 Lyon, France
[8] TGF-β and Immuno-evasion Department of Immunology Virology and Inflammation INSERM U1052, Cancer Research Center of Lyon, F-69000 Lyon, France
[9] Cytometry platform, INSERM U-1052, Cancer Research Center of Lyon, F-69000 Lyon, France
[10] TGF-β and Immuno-evasion, Tumor immunology Program, DKFZ, Heidelberg, Germany
[11] Centre Léon Bérard, « Medical Oncology Department», Lyon, F-69008, France

Running title: Autocrine Ado regulates polyfunctional $CD73^+CD4^+$ T cells

***To whom correspondence should be addressed:** Christine Ménétrier-Caux, Phone (+33) 4-78-78-27-50; e-mail address: christine.caux@lyon.unicancer.fr

No Conflict of Interest to disclose

Abstract

The production of CD73-derived Adenosine (Ado) by Tregs, has been proposed as a resistance mechanism to anti-PD1 therapy in murine tumor models. We reported that

Human Tregs express the ecto-nucleotidase CD39, that generates AMP from ATP, but do not express the AMPase CD73. In contrast, CD73 defined a subset of effector $CD4^+$ T cells (Teffs), enriched in polyfunctional Th1.17 cells characterized by expression of CXCR3, CCR6 and MDR1 and production of IL-17A/IFN-γ/IL-22/GM-CSF. $CD39^+$ Tregs selectively targeted $CD73^+$ Teffs through cooperative degradation of ATP into Ado inhibiting and restricting the ability of $CD73^+$ Teffs to secrete IL-17A.

$CD73^+$ Teffs infiltrating breast and ovarian tumors, were functionally blunted by Tregs expressing upregulated levels of CD39 and ATPase activity. Moreover, tumor-infiltrating $CD73^+$ Teffs failed to express inhibitory immune checkpoints suggesting that CD73 might be selected under pressure from immune checkpoint blockade therapy and thus may represent a non-redundant target for restoring antitumor immunity.

Edited significance: Polyfunctional $CD73^+$ T cell effectors lacking other immune checkpoints are selectively targeted by CD39 overexpressing Tregs that dominate the breast tumor environment.

Introduction

During infection or tumor development, adenosine triphosphate (ATP) is released into the extracellular space and can be found at high levels in inflamed tissues, including tumors (1). Extracellular ATP represents a pro-inflammatory alarmin for the immune system. It induces the chemo-attraction of dendritic cells (DC) and the activation of inflammasomes and IL-1β secretion by monocytes/macrophages (Mφ) through the engagement of P2 purinergic receptors (for review: (2)). Interestingly, the degradation of ATP into adenosine (Ado) by murine $CD4^+$ regulatory T cells (Tregs), co-expressing CD39 and CD73, has been associated with immunosuppression (3), particularly within tumor environment (4, 5). Mechanistically, CD39 (ectonucleoside triphosphate diphosphohydrolase-1, ENTPD1) degrades ATP and adenosine diphosphate (ADP) into adenosine monophosphate (AMP), which is then hydrolyzed by CD73 (5'-ectonucleotidase, NT5E) into Ado. Ado can favor tumor progression by inhibiting the function of immune cells (T cells, monocytes, DCs, Mφ), through the engagement of its receptors (AdoR) A2a or A2b (for review: (6)). These AdoR induce an increased concentration of intracellular cyclic AMP, resulting in the inhibition of proliferation, cytotoxic functions and cytokine secretion (IL-2, TNF-α, IFN-γ and IL-13) of T

cells (for review: (6)). Ado can act also on innate immune cells by inhibiting IL-12 production by DCs (7, 8), and inducing IL-10 and VEGF secretion by Mφ which favor immunosuppression and angiogenesis (9, 10). Moreover, Ado can act on non-immune cells, such as tumor cells, through A1 or A3 receptors coupled to Gαi proteins, fostering tumor cell proliferation and migration (for review: (6)). The importance of Ado signaling in immunosuppression is evidenced in patients with Severe Combined Immunodeficiency (SCID), in whom accumulation of Ado, due to a lack of adenosine deaminase (ADA) enzyme that degrades Ado into Inosine, is observed (11). Remarkably, in CD73-deficient mice, in mice with CD73-deficient Tregs, or in A2a-deficient mice, the antitumor immune response is increased, leading to the tumor rejection and to the inhibition of metastases (12-15). Also, in murine models, targeting of CD73 alone or in combination with immunotherapy (anti-CTLA-4 or anti-PD-1) enhances tumor rejection and blocks metastases, demonstrating that endogenous Ado limits the efficacy of these immunotherapies (16, 17).

Studies investigating the expression of CD73 and CD39 on human T cells subsets remain scarce. In fact, despite the poor prognostic value of Tregs in breast and ovarian tumors (18, 19), the co-expression of CD39 and CD73 on human Tregs remains controversial (20-23). A recent report by Doherty *et al* also suggests the interconnection between CD73 expression on memory $CD4^+$ T cells and a Th17 profile (24).

Th17 cells, implicated in the response to extracellular pathogens, are characterized by the secretion of IL-17A, IL-17F and IL-22. Recently, the involvement of a subset of Th17 cells, called Th1.17 co-producing IL-17A, IFN-γ and GM-CSF, in the development of autoimmune diseases, was unveiled (25), highlighting the polyfunctionality of these cells (26, 27). In tumor biology, a pro-tumoral role of Th17 was reported and mainly associated with the secretion of IL-17A, however, co-production of IFN-γ and GM-CSF was not considered, except in a recent report, demonstrating that Th1.17 cell subset contributes to tumor rejection (28).

In the present work, we demonstrate that CD73, not detected on human Tregs, defines a subpopulation of $CD4^+$ effector T cells (Teffs) associated with cytokine polyfunctionality similar to that described in Th1.17 cells. $CD73^+CD4^+$ Teffs cooperate with $CD39^+$ Tregs to degrade ATP into immunosuppressive Ado inhibiting and restricting function of $CD73^+CD4^+$ Teffs to IL-17A secretion. This cooperation does not require cell contact and, in a spaced-out microenvironment, induces specific inhibition of $CD73^+CD4^+$ Teffs through autocrine ATP-

derived Ado action without affecting distant $CD73^{neg}CD4^{+}$ Teffs. Interestingly, we reveal that $CD73^{+}CD4^{+}$ Teffs are present in breast and ovarian tumor environment together with $CD39^{high}$ Tregs and express only low levels of inhibitory immune checkpoints (i-ICPs) highlighting CD73 as a potential resistance mechanism to current immunotherapies, and as a non-redundant target for restoring antitumor immunity.

Material and methods

Human samples

HD-blood was purchased anonymously from the French Blood Service (EFS). In addition, blood and primary tumor samples were obtained from patients with non-pretreated breast tumors and chemotherapy-pretreated ovarian tumors. All of these samples were provided by the tissue bank (BRC) of Léon Bérard Cancer Center (CLB), after approval from the institutional review board and ethics committee (L-06-36 and L-11-26) and patients' written informed consent, in accordance with the Declaration of Helsinki. Human healthy colon endoscopic biopsies obtained during routine endoscopic check-ups of healthy donors selected on the basis that they were neither under chemotherapy nor taking antibiotics were obtained from the BRC of the CLB after approval from the institutional review board and ethics committee (French agreement number: AC-2013-1871) and donors' written informed consent.

Purification of the different cell subsets

PBMC were purified from blood of HDs or cancer patients by Ficoll density gradient. Memory $CD4^{+}$ T cells were purified using MagniSort™ Human $CD4^{+}$ Memory T Cell Enrichment Kit (eBioscience). $CD73^{neg}CD4^{+}$ Teffs ($CD4^{+}CD45RA^{neg}CD127^{+}CD25^{neg}$ $CD39^{neg}CD73^{neg}$), $CD73^{+}CD4^{+}$ Teffs ($CD4^{+}CD45RA^{neg}CD127^{+}CD25^{neg}CD39^{neg}CD73^{+}$) and total Tregs ($CD4^{+}CD45RA^{neg}CD127^{neg}CD25^{+}$) or $CD39^{+}$ and $CD39^{neg}$ Treg subsets were sorted from purified memory $CD4^{+}$ T cells by multi-parametric FC (FACSAria III, BD Biosciences) using antibodies against CD25 (2A3, BD-Biosciences), CD45RA (2H4LDH11LDB9, Beckman-Coulter), as well as CD127 (eBioRDR5), CD39 (eBioA1) and CD73 (AD2) (all from eBioscience), alongside a viability marker (DAPI). Infiltrating $CD4^{+}$ T cells from breast and ovarian tumors and healthy colonic tissues were isolated from single cell suspensions, obtained by enzymatic disaggregation (18), with the Dynabeads Human $CD4^{+}$ Kit (Life Technologies).

Tumor-infiltrating $CD4^+$ Teffs ($CD127^+CD25^{neg}$) and Tregs ($CD127^{neg}CD25^+$) were sorted from single cell suspensions by multi-parametric FC using antibodies against CD127, CD25, CD45RA, and a viability marker (Fixable Viability Dye, Biolegend).

Flow cytometry analyses

Multi-parametric FC analyses were performed on i) PBMC from HDs or cancer patients, or on ii) single cell suspensions derived either from primary breast and ovarian tumors or healthy colonic tissues. The FC panels used to assess T cell differentiation relied on the use of anti-human antibodies against CD3 (UCHT1), CD4 (RPA-T4), CD8 (SK1), CD95 (DX2) and CD28 (CD28.2) (all from BD-Biosciences), CD27 (O323, eBioscience), CCR7 (G043H7, Biolegend), CD45RA, CD39 and CD73 (see above), while those used to evaluate T cell polarization relied on the use of the anti-human antibodies against CD3, CD4, CD45RA, CD127, CD25, CD39 and CD73 (see above), CCR6 (11A9, BD-Biosciences), CXCR3 (G025H7) and CRTH2 (BM16) from Biolegend, and a viability marker. The i-ICPs panel included antibodies against CD3, CD4, CD8 (see above), CD45 (HI30), PD-1 (EH12.1), TIM-3 (7D3) (all from BD-Biosciences), CD45RA (HI100) and CTLA-4 (L3D10) (Biolegend), TIGIT (MBSA43), CD39 and CD73 (eBioscience) and a fixable viability marker (Zombie Fixable Viability Dyes, Biolegend). The production of intracellular cytokines on $CD73^+CD4^+$ and $CD73^{neg}CD4^+$ Teffs was analyzed using the test previously described (29) with some modifications, in particular the evaluation of IL-22 (22URTI, BD-Biosciences) instead of IL-21. Cells were analyzed on a LSR-Fortessa (BD Biosciences) and data were processed using the FlowJo Software (Tree Star). For the co-expression of i-ICPs, data were analyzed using the Boolean method on the FlowJo software and then represented using SPICE v5.3 software.

MDR1 staining and activity assay

Purified memory $CD4^+$ T cells were incubated with Rh123 (1µg/ml, Sigma-Aldrich) for 30 min on ice. After washes in PBS, cells were incubated at 37°C for 2h efflux phase. Cells were then washed in PBS and stained with surface markers for FC analysis. In some conditions, a MDR1 inhibitor, Elacridar (1µM, Tocris), or vehicle (DMSO) were added to cells immediately before the efflux phase. MDR1 expression was assessed using an anti-human MDR1 antibody (UIC2, eBioscience) for 20 min at 37°C in the presence of Cyclosporin A (25 µM, R&D Systems), as described previously (30).

Transcriptomic analyses

$CD73^{neg}$ and $CD73^{+}$ $CD4^{+}$ Teffs were sorted from the PBMC of six HDs blood samples. Cells were activated in the presence of anti-CD3/anti-CD28 beads (Expand beads, Life Technologies, ratio 1 bead to 4 cells) in complete RPMI medium (supplemented with antibiotics, L-glutamine (Life Technologies) and 5% of human serum AB^{+} (EFS)) at 37°C under 5% CO_2. Resting and short-term activated cells (mix of 6 hours and 24 hours activation), were lyzed for mRNA extraction (miRNeasy micro Kit, Qiagen) and transcriptomic analyses (Human Gene-Expression 8x60K Microarray Kit AMADID 039494, Agilent Technologies) were performed.

Western blot analyses

Tregs, $CD73^{neg}$ or $CD73^{+}$ $CD4^{+}$ Teffs ($2x10^{6}$ cells) were isolated and lyzed in RIPA-Buffer in the presence of proteinase inhibitors. Protein lysates were boiled, loaded on Mini-PROTEAN® TGX™ Precast Gels 5-20% (Biorad) and transferred to Trans-Blot® Turbo™ Mini PVDF membrane (Biorad). CD73 was detected using a mouse anti-hCD73 antibody (1D7, 1/500, Abcam). Pellets of MDA-MB231 cell line (LGC Standards) whose genetic profile has been verified (Eurofins Forensic Department) and negative for mycoplasma (MycoAlert mycoplasma detection kit, Lonza) and human purified HD blood monocytes were used as positive and negative control, respectively. ADA and A2b receptors were assessed either on purified $CD73^{neg}$ or $CD73^{+}$ $CD4^{+}$ Teffs, or after 1 or 4 days activation with Expand beads (ratio 1:4), using a goat anti-A2bR antibody (ab40002, 1/1000, Abcam) and a mouse anti-hADA antibody (ab54969, 1/500, Abcam). The HRP-coupled secondary antibodies used were goat anti-mouse Ab (12-349, 1/5000, Upstate), rabbit anti-goat Ab (P 0449 1/2000, Dako). Membranes were revealed with Luminata Crescendo Reagent (Millipore) and analyzed on Chemidocs™ system (Biorad).

Proliferation experiments

$CD73^{neg}CD4^{+}$ and $CD73^{+}CD4^{+}$ Teffs were stained respectively with the carboxyfluorescein succinimidyl ester (CFSE) (2 µM, Life Technologies) and CellTrace Violet (CTV) (20 µM, Life Technologies) proliferation markers, while Tregs were co-stained with both CFSE and CTV according to manufacturer's instructions. $CD73^{neg}CD4^{+}$ Teffs or $CD73^{+}$ $CD4^{+}$ Teffs ($3x10^{4}$) alone, in co-culture with Tregs (total or sorted $CD39^{+}$ and $CD39^{neg}$ subsets) at a ratio 1:1 or co-culture of $CD73^{neg}CD4^{+}$ Teffs, $CD73^{+}CD4^{+}$ Teffs and Tregs at physiological ratio

(70%:20%:10%) were incubated with Expand beads (ratio 1:4) in 96-round-bottomed-well plates (Falcon) in 200 µl of complete RPMI medium for 4 days at 37°C under 5% CO_2. Ado, AMP, or ATP (Sigma-Aldrich) were added every day at the indicated concentration, whereas the CD73 inhibitor (APCP, 50 µM, Sigma-Aldrich), CD39 inhibitor (ARL-67156, 250 µM, Tocris) or rhADA (1 µg/ml, R&D Systems) were pre-incubated for 30 minutes before the beginning of the culture. At the end of the experimental time-course, cells were harvested and stained with a viability marker (LIVE/DEAD® Fixable Dead Cell Stains) and fixed in 2% formaldehyde. Cell proliferation was analyzed under an inverted Zeiss microscope (Objective 4x) using an Axiovision 4 software (Zeiss), and by FC (LSR Fortessa, BD Biosciences) according to the CFSE and CTV dilution.

For experiments in Transwell Permeable Supports (polycarbonate membrane 0.4 µm pore Corning), in the 6.5 mm inserts, $6x10^4$ $CD73^+CD4^+$ Teffs alone or in co-culture with Tregs (at a ratio of 1:1) were activated using Expand beads (ratio of 1:4) in the presence, in the bottom wells, of $1.5x10^5$ $CD73^{neg}CD4^+$ Teffs alone, or in co-culture with Tregs (at a ratio of 1:4) and Expand beads (ratio 1:4), in a total volume of 800 µl.

Cytokines analysis

$CD73^{neg}CD4^+$ or $CD73^+CD4^+$ Teffs ($5x10^4$) were activated with either PMA (50ng/ml)/Ionomcycin (1µg/ml) (Sigma-Aldrich) for 24 hours or Expand beads (ratio of 1:4) for 48 hours in complete RPMI at 37°C under 5% CO_2, and in the presence or not of Ado (75µM or 100µM). Supernatants were harvested and frozen, and cytokines were analyzed by ELISA using Luminex Multiplex Kits (eBioscience) (Multiplex 1: IL-2/TNF-α/IFN-γ/IL-22/IL-17A/IL-10/IL-13/IL-21; Multiplex 2: GM-CSF/IL-3).

Nucleotides and nucleosides quantification by HPLC coupled to LC-MS/MS

The capacity of $5x10^4$ Tregs, $CD73^{neg}CD4^+$ Teffs or $CD73^+CD4^+$ Teffs alone or co-culture of Tregs with either $CD73^{neg}CD4^+$ Teffs or $CD73^+CD4^+$ Teffs (ratio 1:1), to degrade ATP or AMP was analyzed after 2 hours incubation at 37°C under 5% CO_2 with labeled $ATP_{13C,15N}$ or $AMP_{13C,15N}$ (all from Sigma- Aldrich) in 200 µL of serum-free RPMI medium supplemented with antibiotics and L-glutamine (Life Technologies). In some cases, cells were pre-incubated with ARL-67156 (250 µM) or APCP (50 µM) for 30 minutes before the experiment. Cell supernatants were harvested, boiled at 65°C for 5 seconds and frozen at -20°C. $ATP_{13C,15N}$,

$AMP_{13C,15N}$, $Ado_{13C,15N}$ and $Inosine_{13C,15N}$ were quantified in 50 µl of supernatant. Nucleotides and nucleosides were extracted using off-line Oasis-WAX® cartridges (60 mg; 3 cc). Briefly, cartridges were conditioned using 2 ml of methanol and 2 ml of water. After sample loading, cartridges were washed with 1 ml of water. Elution was performed thrice using 1 ml of the following mixture: NH_4OH 0.25% pH 10.0/water/acetonitrile (30/30/40, v/v). Eluates were pooled and gas dried under nitrogen at 37°C. The residue was suspended in 250 µl of 5mM HA-0.5% DEA in water, and 10 µl were injected into a liquid chromatograph.

Analysis was performed using liquid chromatography coupled with a tandem mass spectrometer (LC-MS/MS) as previously described by Machon *et al* (31). Quantification was conducted by adding standard solutions of labelled nucleotides (ATP_{13C}, AMP_{15N}, Ado_{13C} and $Inosine_{15N}$) to samples prior to the extraction step. ATP_{15N} and $GMP_{13C,15N}$ were used as internal standards. Concentrations of nucleotides in the supernatants were calculated using calibration curves of the corresponding labelled nucleotides. We also verified that ARL-67156 (250 µM) and APCP (50 µM) did not interfere with the ATP, AMP, Ado and Inosine quantification.

Multi-immunofluorescence stainings on frozen tumor sections

Tissue-Tek® O.C.T. (Sakura® Finetek) embedded frozen human primary breast tumors were used to generate 6 µm frozen tissue sections with Cryotome™ (Thermo Fisher Scientific). Sections were fixed in paraformaldehyde, permeabilized in Triton X-100 and stained with murine anti-human CD4-AF488 (Biolegend, Clone RPA-T4), rat anti-human FoxP3-APC (Ebioscience, Clone PCH101), and uncoupled rabbit anti-human CD73 (Cell signalling, Clone D7F9A). CD73 staining was revealed with secondary Donkey anti-rabbit antibody (Life Technologies). Immunofluorescence stainings were analyzed on Upright Microscope (Nikon Ni-E) using ImageJ free software.

Results

CD39 and CD73 are expressed by distinct memory $CD4^+$ T cells in humans

We initially observed by flow cytometry (FC), that human $CD4^+$ T cells in the blood of healthy donors (HD-blood) did not co-express CD39 and CD73 but exclusive $CD39^+$ or $CD73^+$ cells were observed among $CD4^+$ T cell populations (**Fig. 1A**). While naive $CD4^+$ T cells expressed no or very low levels of CD39 and CD73 (**Fig. 1A, B**), the expression of CD39 and CD73 was detectable on memory $CD4^+$ T cells (**Fig. 1A**). Among memory $CD4^+$ T cells, CD39, but not

CD73, was expressed at variable levels on human HD-blood Tregs defined by FoxP3 expression (**Fig. 1A, C**). The absence of CD73 expression on Tregs purified from blood was also confirmed by western blot analysis (**Fig. 1D**). In contrast, CD73, but also CD39, can be expressed on distinct populations of $CD4^+$ Teffs defined by the absence of FoxP3 expression (**Fig. 1A, E**). Of note, the intensity of CD73 expression on $CD73^+CD4^+$ Teffs was significantly higher compared to naive $CD73^+CD4^+$ T cells (**Fig. 1F**). Moreover, the percentage and the intensity of CD39 expression was lower on $CD4^+$ Teffs compared to Tregs (Δ CD39 MFI Tregs/ $CD4^+$ Teffs: 1.64 ± 0.33).

Our results demonstrate that in contrast to murine Tregs, human Tregs only express CD39. They also highlight the expression of CD73 on a subset of $CD4^+$ Teffs. Thus, we wondered whether the expression of CD73, favoring the generation of Ado, on a subset of $CD4^+$ Teffs may denote a functional specialization of this population.

CD73 identifies a population of $CD4^+$ Teffs enriched in polyfunctional Th1.17 cells

We analyzed by FC the expression pattern of the chemoattractant receptors CRTH2, CXCR3 and CCR6 on blood $CD73^+$ versus $CD73^{neg}$ $CD4^+$ Teffs in order to determine the relative percentage of Th1 ($CRTH2^{neg}CXCR3^+CCR6^{neg}$), Th2 ($CRTH2^+CXCR3^{neg}CCR6^{neg}$), Th17 ($CRTH2^{neg}CXCR3^{neg}CCR6^+$) and Th1.Th17 ($CRTH2^{neg}CXCR3^+CCR6^+$) (26) (**Fig. S1A**). $CD73^+CD4^+$ Teffs contained a similar proportion of Th1, Th17 and Th2 subsets as $CD73^{neg}$ Teffs, but exhibited an increased proportion of the Th1.17 subset, which accounted for 27.98 ± 7.99 % of total cells, at the expense of other Th cells (**Fig. S1B, Fig. 2A**). Consistent with this Th1.17 enrichment, a higher proportion of $CD73^+CD4^+$ Teffs migrated toward a CXCL10 or CCL20 gradient in Transwell chemotaxis assays (**Fig. S1C**). Analysis of the transcriptome of purified $CD73^+$ and $CD73^{neg}$ $CD4^+$ Teffs after short term TCR stimulation revealed an overexpression of Th1.17-related genes (*CSF2, ABCB1, IL22, IL3, IFNG, GZMB, IL23R, TBX21, LGALS3*) (25, 27) in the former subset, while genes related to Th2 cells (*IL4, IL10, IL13, CCR4*) and Th17, Tfh or Tr1 (*LRMP, IKZF3, CXCR5, IL21, IL10*) were downregulated (**Fig. 2B**). IL-17A and IL-17F gene were not detected likely due to insufficient sensitivity of transcriptomic chip used in our conditions.

We also performed short-term *in vitro* reactivation of PBMC with PMA/ionomycin to analyze cytokines production by intra-cytoplasmic staining in $CD73^+$ *versus* $CD73^{neg}$ $CD4^+$ Teffs. We found a higher proportion of cells producing IL-2, TNF-α, IL-17A, IFN-γ, IL-22, in $CD73^+$ $CD4^+$

Teffs (**Fig. 2C**). More precisely, $CD73^+CD4^+$ Teffs were enriched in cells co-producing IFNγ/IL-17A (**Fig. 2C**). A multiplex immunoassay performed with supernatants of these *in vitro* activated subsets confirmed the significantly increased production of all cytokines but also of IL-3 and GM-CSF by $CD73^+CD4^+$ Teffs (**Fig. 2D**) except IL-2 analyzed by FC (**Fig. 2C**). In addition, this assay revealed the low production of IL-10, IL-13 and IL-21 (**Fig. 2D**) compared to $CD73^{neg}CD4^+$ Teffs in accordance with Th1.17 gene signature (**Fig. 2B**).

One of the most upregulated genes differentiating $CD73^+$ and $CD73^{neg}$ $CD4^+$ Teffs (**Fig. 2B**) after *CSF2* gene (coding for GM-CSF) is the *ABCB1* gene, coding for the multidrug transporter MDR1 and recently proposed as a Th1.17 specific marker (27). A significantly increased expression of MDR1 on $CD73^+CD4^+$ Teffs compared to $CD73^{neg}CD4^+$ ones was observed at the protein level by FC (**Fig. 2E**) and at the functional level with the Rh123 exclusion assay (**Fig. 2E**, **Fig. S1D**).

Taken together, our results demonstrate that CD73 identifies a subset of $CD4^+$ Teffs enriched in polyfunctional Th1.17 cells. Consistent with this conclusion, a high proportion of $CD73^+CD4^+$ Teffs was observed in the colon of healthy individuals (**Fig. 2F**), a mucosal tissue known to be enriched in Th17 and Th1.17 populations (32).

$CD73^+CD4^+$ Teffs cooperate with $CD39^+$ Tregs for Ado production

Next, we evaluated the capacity of $CD73^+CD4^+$ Teffs to generate Ado from AMP through the measurement of nucleotides and nucleosides by HPLC (31). AMP degradation and generation of Ado were observed after 2-hours incubation with AMP and were abrogated by a specific CD73 inhibitor (**Fig. 3A**). Whereas purified human $CD73^+CD4^+$ or $CD73^{neg}CD4^+$ Teffs were not able to degrade ATP (**Fig. 3B**), purified human Tregs were able to degrade 48.24 ± 6.20% of ATP into AMP without generation of Ado (**Fig. 3B**). We confirmed that degradation of ATP results from CD39 expression by Tregs as only purified $CD39^+$ Tregs but not $CD39^{neg}$ Tregs generated AMP and that ATP degradation was blocked by a CD39 inhibitor (**Fig.3C**). The addition of purified $CD73^+CD4^+$ Teffs with Tregs favored the generation of Ado following ATP degradation (**Fig. 3B**).

Ado suppresses proliferation and restricts polyfunctional $CD73^+CD4^+$ Teffs to IL-17A secretion

The capacity of $CD73^+CD4^+$ Teffs to generate Ado suggests that these cells may be particularly sensitive to Ado. This immunosuppressive molecule exerts its immuno-suppressive functions by engaging A2a or A2b receptors but can be degraded into Inosine by the enzyme ADA. Our transcriptomic data revealed that *ADORA2A,* but not *ADORA2B*, was expressed on resting $CD73^+$ and $CD73^{neg}$ $CD4^+$ Teffs, and that both receptors were upregulated following short-term TCR triggering (**Fig. 4A**). In contrast, *ADORA1* (*A1R*) and *ADORA3* (*A3R*) were not detected as described in the literature (6). *ADA* mRNA expressed at steady state, decreased after activation on both subsets (**Fig. 4A**). The modulation observed for *ADORA2B* and *ADA* at mRNA level was confirmed at the protein level, which gradually increased for A2bR and decreased for ADA until 4 days of activation (**Fig. 4B**). These data demonstrated the acquisition of an Ado-sensitive phenotype by $CD73^+$ and $CD73^{neg}$ $CD4^+$ Teffs upon TCR triggering, as observed in the murine model (3). Otherwise, no significant difference in the cell-proliferation capacities of both subsets were observed using same proliferation markers evaluated by FC (**Fig. S1E**).

The metronomic addition of exogenous Ado (75 µM/day) inhibited the proliferation of both subsets as shown by the reduction of cell clusters size (round bottomed well observation, (**Fig. 4C**) and dilution of the CTV proliferation marker (**Fig. S2**) compared to the medium condition. The addition of recombinant ADA (rhADA, 1 µg/ml), restored the proliferative capacity of both T cell subsets (**Fig. 4C**, **Fig. S2**).

The impact of Ado was also analyzed on the cytokines production capacity of both purified $CD4^+$ Teffs subsets. To avoid any confounding effects of Ado on proliferation, cytokine secretions were analyzed after 2 days of TCR triggering, determined as the optimal time lapse for cell activation without proliferation. Of great interest, Ado significantly inhibited the secretion of most of the cytokines produced by $CD73^+CD4^+$ Teffs except IL-17A and only a slight effect was observed on IL-22 secretion (**Fig. 4D**).

These results indicate that Ado suppresses the proliferation of both subsets in the same manner but dramatically restricts the functionality of $CD73^+CD4^+$ Teffs to IL-17A production.

CD39$^+$ Tregs make CD73$^+$CD4$^+$ Teffs sensitive to ATP-derived Ado in spaced-out environment.

We previously observed that CD73$^+$CD4$^+$ Teffs were able to generate Ado from AMP produced by the ATP degradation from CD39$^+$ Tregs (**Fig. 3**). Moreover, we found that functional CD73 on CD4$^+$ Teffs favored their suppression mediated by AMP-derived Ado similar to that observed in presence of exogenous Ado (**Fig.S3A, S3B**). We then analyzed the biological impact of the cooperation between CD39$^+$ Tregs and CD73$^+$CD4$^+$ Teffs, by co-culturing Tregs with purified CD73$^+$ or CD73^{neg} CD4$^+$ Teffs in presence or absence of exogenous ATP. As previously reported (18, 33), Tregs did not present any sign of proliferation, due to their anergic status. Conversely, the proliferation of purified CD73$^+$ or CD73^{neg} CD4$^+$ Teffs was unaltered by the addition of Tregs, due to the strong TCR triggering signal. Although ATP alone did not modulate the proliferation of either CD4$^+$ Teffs subpopulations, combination of Tregs and ATP strongly suppressed the proliferation of CD73$^+$CD4$^+$ Teffs, but not CD73^{neg}CD4$^+$ Teffs. This inhibition was reversed by the addition of inhibitors of CD73 (APCP) or CD39 (ARL67156) (**Fig. 5A**, **Fig. S4**).

Similar suppression experiments performed with Treg subsets sorted based on CD39 expression confirmed that CD39$^+$ Tregs but not CD39^{neg} ones suppressed specifically the proliferation of CD73$^+$CD4$^+$Teffs in presence of exogenous ATP (**Fig. 5B**).

Transwell experiments enabled us to address the importance of the co-localization of CD73$^+$CD4$^+$ Teffs and Tregs in this Ado-mediated suppression. CD73$^+$CD4$^+$ Teffs were cultured in the upper chamber and CD73^{neg}CD4$^+$ Teffs in the lower one, whereas Tregs were added in either one or the other. The addition of exogenous ATP, whatever the localization of Tregs, induced a strong inhibition of CD73$^+$CD4$^+$ Teffs proliferation, indicating that the co-localization of CD73$^+$CD4$^+$ Teffs and Tregs is not necessary to obtain ATP-mediated inhibition of CD73$^+$CD4$^+$ Teffs (**Fig. 5C**).

Of importance, these experiments revealed that the proliferation of CD73^{neg}CD4$^+$ Teffs localized in the lower chamber was not altered by Ado generated by CD73$^+$CD4$^+$ Teffs in the upper one demonstrating that CD73$^+$ cells among CD4$^+$ Teffs were preferentially inhibited by Tregs through Ado generation (**Fig. 5C**). As Ado similarly inhibited purified CD73^{neg} or CD73$^+$ CD4$^+$ Teffs in 'U' wells (**Fig. 4C**) and in Transwell (**Fig. 5C**), we addressed the importance of both CD4$^+$ Teffs populations co-localization for Ado-mediated inhibition resulting from ATP degradation. In cultures where Tregs, CD73$^+$CD4$^+$ Teffs and CD73^{neg} CD4$^+$ Teffs, mixed at

physiological ratio observed in blood (10%/20%/70%), were co-localized altogether in "U" wells, the $CD73^{+}CD4^{+}$ Teffs subset was suppressed by autocrine generation of Ado through collaboration with Tregs, but the $CD73^{neg}$ population was also suppressed by paracrine action of generated Ado (**Fig. 5C, D, E**). This demonstrated that, in a culture system favoring close interactions between T cell subsets, cooperation of Tregs and $CD73^{+}CD4^{+}$ Teffs degrading ATP into Ado, inhibited proliferation of $CD73^{+}CD4^{+}$ Teffs but also surrounding $CD73^{neg}CD4^{+}$ Teffs.

Collectively, these data highlight that the cooperation between Tregs and $CD73^{+}CD4^{+}$ Teffs does not require cell-contact. Furthermore, Ado, acting in an autocrine manner on $CD73^{+}CD4^{+}$ Teffs, does not affect the proliferation of $CD73^{neg}CD4^{+}$ Teffs except if they are co-localized at high cell density, through collateral paracrine effect. Altogether our data suggest that the $CD73^{+}$ population among $CD4^{+}$ Teffs is selectively targeted by $CD39^{+}$ Tregs through autocrine Ado production.

$CD73^{+}CD4^{+}$ Teffs are present in the tumor microenvironment enriched in $CD39^{+}$ Tregs

We analyzed $CD73^{+}CD4^{+}$ Teffs and $CD39^{+}$ Tregs in patients with primary Breast (BT) or Ovarian (OT) tumors. The frequency of memory cells among $CD4^{+}$ T cells (**Fig. S5A**), Tregs among memory $CD4^{+}$ T cells (**Fig. S5B**), and the CD39/CD73 expression pattern on Tregs and $CD4^{+}$ Teffs in BT- or OT-blood were similar to that observed in healthy donors (**Fig. 6A, B**). However, in contrast to that observed on $CD4^{+}$ Teffs, the percentage and intensity of CD39 on Tregs tended to increase in BT-blood (62.31 ± 14.94%) and OT-blood (62.79 ± 14.93%), compared to HD-blood (50.01 ± 24.88%). Conversely, there was no modulation of $CD73^{+}CD4^{+}$ Teffs proportion (**Fig. S5C**), cytokine production pattern (**Fig. S5D**) or Rh123 efflux capacity (*Bossennec, in preparation*), in the blood of cancer patients.

In breast and ovarian tumor tissues, we observed a strong enrichment of memory cells among $CD4^{+}$ T cells (**Fig. S5A**) and of Tregs among memory $CD4^{+}$ T cells, which frequency reached roughly 3-times that found in patient's blood as previously reported by our team (18) and others (19). In the BT and OT microenvironment, as observed in blood, Tregs expressed CD39 but not CD73 (**Fig. 6A**). Interestingly, the percentage of $CD39^{+}$ Tregs was also increased, leading to an increase of $CD39^{+}$ Tregs frequency among total $CD4^{+}$ T cells of about four fold compared to blood. Finally, the intensity of CD39 expression was also

significantly higher in BT and OT compared to matched blood (**Fig. 6C, D**). In addition, CD39 expression on tumor-infiltrating Tregs was higher than on $CD4^+$ Teffs in terms of percentage and intensity of expression (**Fig. 6E, F**). The upregulated CD39 expression on tumor Tregs compared to blood Tregs was associated to an increased capacity to degrade exogenous ATP into AMP (**Fig. 6G**). In contrast, the proportion of $CD73^+CD4^+$ Teffs was not significantly modulated in the tumor microenvironment (BT: 4.74 ± 2.64%; OT: 4.73 ± 2.71%) compared to blood (HD-blood: 7.37 ± 3.21%) (**Fig. 6B, H**). Tumor-infiltrating $CD73^+CD4^+$ Teffs, activated with PMA/ionomycin, presented a higher percentage of IL-2, TNF-α, IFN-γ, IL-17A producers, and IFN-γ/IL-17A co-producers compared to the $CD73^{neg}CD4^+$ Teffs (**Fig. 6I**), as observed in BT- and OT-blood (**Fig. S5D**) and HD blood (**Fig. 2D**). Multi-Immunofluorescence stainings on primary BT frozen sections confirmed the co-detection of Tregs ($FoxP3^+$) and $CD73^+CD4^+$ Teffs within the stromal immune infiltrate (**Fig. 6J**).

The presence of $CD73^+CD4^+$ Teffs and the enrichment of $CD39^+$ Tregs in BT and OT support the idea that in breast and ovarian tumor environments, CD39/CD73-mediated Ado generation can occur and suppress $CD4^+CD73^+$ Teffs activation.

Tumor-infiltrating $CD73^+CD4^+$ Teffs have lower expression of inhibitory immune checkpoints

To determine whether the intrinsic capacity to transform AMP into Ado may constitute the main functional regulatory pathway of $CD73^+CD4^+$ Teffs, we analyzed, by FC, the co-expression of i-ICPs namely TIGIT, CTLA-4, TIM-3 and PD-1 on $CD4^+$ Teffs (**Fig. 7A**). i-ICPs expression was mostly observed on tumor-infiltrating $CD4^+$ T cells compared to paired blood. The relative percentage of $TIGIT^+$ or $PD\text{-}1^+$ cells were significantly lower in $CD73^+$ cells compared to $CD73^{neg}$ ones among $CD4^+$ Teffs from tumor tissues (**Fig. 7A, B**). Indeed, tumor-infiltrating $CD73^+CD4^+$ Teffs contained higher proportion of cells devoid of i-ICPs and fewer cells co-expressing 2, 3 or 4 i-ICPs, compared to $CD73^{neg}CD4^+$ Teffs (**Fig. 7C**). Moreover, the intensity of PD-1 expression was lower on tumor-infiltrating $CD73^+CD4^+$ Teffs compared to $CD73^{neg}CD4^+$ Teffs (**Fig. 7D**).

These findings, associated with the previous evidence that $CD73^+CD4^+$ Teffs are functionally suppressed by autocrine Ado generated through cooperation with $CD39^+$ Tregs, strongly suggest that the CD39/CD73/Ado pathway might constitute the main pathway controlling the Th1.17 potency of human $CD73^+CD4^+$ Teffs.

Consistent with this conclusion, analyses done on PD-1 expressing $CD4^+$ tumor-infiltrating T cells in BT and OT unveils that, the proportion of cells devoid of i-ICPs was reduced to 7% among BT-infiltrating $PD1^+CD4^+$ Teff (and 15,5% for OT) contrasting with more than 63% among BT-infiltrating $CD73^+CD4^+$ Teffs (and 46,8 for OT) (**Fig. S5E)**.

Discussion

We have herein demonstrated that CD73 expression on $CD4^+$ T cells delineates polyfunctional memory $CD4^+$ Teffs enriched in Th1.17 cells whereas Tregs are devoid of CD73 expression. $CD73^+CD4^+$ Teffs are targeted by $CD39^+$ Tregs through ATP degradation into Ado inhibiting and restricting their functionality to IL-17A secretion. This contact independent cooperation induces specific inhibition of $CD73^+$ cells among $CD4^+$ Teffs in a spaced-out environment. In breast and ovarian tumor environments, the increased proportion of Tregs overexpressing CD39 and the presence of $CD73^+CD4^+$ Teffs almost devoid of i-ICPs strongly suggest that CD73-mediated generation of autocrine Ado represents an essential regulatory mechanism of these potent $CD4^+$ Teffs.

Our results highlight that, compared to $CD73^{neg}CD4^+$ Teffs, the $CD73^+$ subset secretes higher levels of pro-inflammatory cytokines (IL-17A, IFN-γ, GM-CSF, IL-22, TNF-α, IL-2, IL-3), and lower levels of anti-inflammatory ones (IL-10, IL-13, IL-21). Of importance, FC analyses reveal the higher propensity of $CD73^+CD4^+$ Teffs to co-produce IFN-γ and IL-17A and co-express CXCR3/CCR6, in line with Th1.17 compared to $CD73^{neg}CD4^+$ Teffs. Our results extend the work of Doherty *et al* (24), who identified the memory $CD73^+CD4^+$ T cells as Th17 cells. Indeed, the exploitation of the transcriptome data from Ramesh *et al* (27), comparing $MDR1^+$ and $MDR1^{neg}$ $CD4^+$ memory populations (Gene Expression Omnibus (GEO) repository, accession ID: GSE49702), reveals that *nt5e* mRNA, coding for CD73, is one of the most significantly upregulated genes in the $MDR1^+$ population (Log2-fold change (FC) = 0.867; p value = 0.004). Moreover, $CD73^+CD4^+$ Teffs present a number of features of Th1.17 cells recently described by Ramesh et al (27). They express high level of functional MDR1, secrete IL-3 and GM-CSF and present higher expression of IL-23R in contrast to non-pathogenic Th17 that produce only IL-17A, IL-22, IL-10 and IL-21 (26, 27, 34). Altogether, our data emphasize the poly-functionality of $CD73^+CD4^+$ Teffs and their similarity with Th1.17.

Th1.17 cells are known to play a pathogenic role in autoimmune diseases through their production of IFN-γ and GM-CSF in addition to IL-17A (for review: (35)). While, Th1.17 cells,

also called pathogenic Th17 induced by Gram$^+$ bacteria influence gut anti-tumor immune response in murine models (36), information on the impact of this population in breast and ovarian tumor remains limited. In fact, in patients with invasive breast carcinoma, IL-17A produced by CD4$^+$ T cells positively correlates with a high histological grade and with triple negative molecular subtype, and represents an independent prognostic factor for shorter disease-free survival (37, 38). In line with these observations, neutralization of IL-17 in murine mammary tumor models inhibits tumor growth (39). In contrast, in ovarian carcinoma, the detection of IL-17 within the tumor microenvironment (40), and more precisely the presence of CD4$^+$ T cells co-expressing IL-17 and IFN-γ (41), is associated with a good prognosis. Owing to their capacity to produce IFN-γ, these cells can exert a potent tumor suppressive activity in synergy with IL-17 in order to reprogram recruited neutrophils and myeloid-derived suppressor cells into potent antitumor effectors, and to neutralize the pro-angiogenic effects of IL-17 through the production of the CXCR3 ligand (CXCL10) (41). This is in line with the strong antitumor response associated to Th1.17 cells in murine ovarian tumor model (28, 41).

Of importance, we observe that Ado blocks all cytokines produced by CD73$^+$CD4$^+$ Teffs, except IL-17A. In this context, the analysis of cytokine pattern in 102 human breast and ovarian tumor mechanic disaggregation milieu (STM: soluble tumor milieu) with sensitive method highlight that 51% (n=52) STM were negative for both IL-17A and IFNγ, 28.4% (n=29) contained only IL-17A whereas 18.6% (n=19) contained both IL-17A and IFNγ and 2.9% (n=3) IFNγ only. As CD73$^+$CD4$^+$ Teffs were detected in most tumors at frequency similar to blood and preserve their capacity to co-produce IL-17A and IFNγ upon PMA+Ionomycin activation (**Fig. 6**), these STM data suggest that the level of endogenous Ado production may vary from tumor to tumor, a high level of Ado production leading to IL-17A only, while a low Ado level allowing both IL-17A and IFNγ co-production. Moreover, 87.5% of STM producing both IL-17A and IFNγ contained high concentrations of CXCL10 (>8ng/ml) whereas only 12.5% of those with IL-17A only and none of the other contained significant levels of CXCL10. This represents another argument that IL-17/IFNγ found in STM may be co-produced by CCR6$^+$CXCR3$^+$ Th1.17 CD73$^+$ Teffs. Further analyses remain necessary to confirm this.

Importantly, we demonstrate that in the presence of exogenous ATP, CD39$^+$ Tregs potently inhibit the proliferation and cytokine production of purified CD73$^+$CD4$^+$ Teffs through CD73-dependent Ado generation without impacting CD73^{neg}CD4$^+$ Teffs. These results support the

concept that the potent $CD73^+$ Th1.17 cells are selectively inhibited by $CD39^+$ Tregs, through the cooperative production of Ado in their local microenvironment. The localized effect of Ado can be explained by its short half-life in tissues due to the presence of ADA and specific membrane transporters (42).

High ATP concentrations released in the tumor microenvironment (1) play an important role in the initiation of the immune response, whereas Ado, also found in human tumor environment (43), fosters tumor progression through its immunosuppressive functions (for review: (2)).

In this study, we confirm the increase in Tregs proportion in breast and ovarian tumor environment (18, 19) and demonstrate an overexpression of CD39 on these tumor-infiltrating Tregs (frequency of $CD39^+$ Tregs within total $CD4^+$ T cells, about 4 fold in tumor compared to blood) which efficiently degrades exogenous ATP into AMP. Consequently, $CD73^+CD4^+$ Teffs will be inhibited through autocrine Ado production. These results support the concept that the Th1.17 potency of $CD73^+CD4^+$ effectors can be selectively inhibited by tumor-infiltrating $CD39^+$ Tregs through cooperative Ado production. Others CD39-expressing cells such as Mφ or B cells may also contribute to the regulation of this $CD73^+$CD4 Teffs (44, 45).

Of further relevance for therapy, $CD73^+CD4^+$ Teffs from blood or tumor present a high expression of the functional multidrug transporter MDR1 suggesting their protection from deleterious effects of chemotherapy, thus strengthening the role they could play in the antitumor immunity. This key property could be evaluated through the analysis of the proportion of these $CD73^+CD4^+$ Teffs following neo-adjuvant chemotherapy. Furthermore, $CD73^+CD4^+$ Teffs express very low levels of i-ICPs (PD-1, TIM-3, TIGIT, CTLA-4), suggesting the non-redundancy of i-ICPs and the adenosinergic pathway in the regulation of these cells. These results corroborate recent reports, in murine tumor models, demonstrating that Ado limits the efficacy of immunotherapeutic interventions targeting CTLA-4 or PD-1/PDL-1, and that CD73 neutralization enhances the efficacy of these therapies (16, 17). Thus, CD73-mediated generation of Ado is an important mechanism of regulation of these polyfunctional $CD73^+CD4^+$ Teffs, and may represent a critical resistance mechanism to current immunotherapies (anti-PD1/L1, CTLA-4). These findings should promote the development of combined therapies based on immunotherapies targeting i-ICPs and the neutralization of the enzymatic function of CD73 (46, 47).

Furthermore, clinical investigations are required to evaluate the presence of $CD73^+CD4^+$ Teffs in primary or chemotherapy-treated tumors and their clinical impact on the survival of the patients in association with the presence of $CD39^+$ cells such as Tregs or Mφ.

Acknowledgments

We wish to thank the staff of the core facilities at the Cancer Research Center of Lyon (CRCL) for their technical assistance and the BRC (Biological Resources Centre) of the CLB for providing human samples. Drs P. Guibert, F. Desseigne, M. Sarabi and L. Mais are acknowledged for their clinical expertise. We will also thank Marie Laure Thibult (Innate Pharma) for her assistance for flow cytometry sorting. We are very grateful to Justine Berthet for her help and expertise in the development of multi-IF analysis on breast tumor sections. We would also like to thank Dr. B. Manship for critical reading of the manuscript.

Financial Support

C. Caux, C. Ménétrier-Caux, N. Gourdin, M. Bossennec, B. Dubois and C. Rodriguez were financially supported by the Breast cancer Research Fundation, and grants from the Puy de Dôme comity of the "Ligue Contre le Cancer". J.C. Marie, D Bauché, C. Caux, C. Ménétrier-Caux, B. Dubois, N. Gourdin, M. Bossennec and C. Rodriguez, O. Tredan, I. Durand and N. Chopin were financially supported by the SIRIC project (LYRIC, grant no. INCa_4664). C. Caux, C. Ménétrier-Caux, N. Gourdin, M. Bossennec and C. Rodriguez, P. Romero, C. Jandus and S. Vigano were financially supported by the FP7 European TumAdoR project (grant n° 602200). J.C. Marie, D Bauché, C. Caux were financially supported by the LABEX DEVweCAN (ANR-10-LABX-0061) of the University of Lyon, within the program "Investissements d'Avenir" organized by the French National Research Agency (ANR).

References

1.Pellegatti,P., Raffaghello,L., Bianchi,G., Piccardi,F., Pistoia,V. & Di,V.F. Increased level of extracellular ATP at tumor sites: in vivo imaging with plasma membrane luciferase. *PLoS. One.* **3**:e2599 (2008).

2.Junger,W.G. Immune cell regulation by autocrine purinergic signalling. *Nat. Rev. Immunol.* **11**:201-212 (2011).

3.Deaglio,S. *et al.* Adenosine generation catalyzed by CD39 and CD73 expressed on regulatory T cells mediates immune suppression. *J. Exp. Med.* **204**:1257-1265 (2007).

4.Stagg,J. *et al.* CD73-deficient mice have increased antitumor immunity and are resistant to experimental metastasis. *Cancer Res.* **71**:2892-2900 (2011).

5.Wang,L. *et al.* CD73 has distinct roles in nonhematopoietic and hematopoietic cells to promote tumor growth in mice. *J. Clin. Invest* **121**:2371-2382 (2011).

6.Ohta,A. A Metabolic Immune Checkpoint: Adenosine in Tumor Microenvironment. *Front Immunol.* **7**:109 (2016).

7.Hasko,G. *et al.* Adenosine inhibits IL-12 and TNF-alpha production via adenosine A2a receptor-dependent and independent mechanisms. *FASEB J.* **14**:2065-2074 (2000).

8.Hasko,G., Kuhel,D.G., Salzman,A.L. & Szabo,C. ATP suppression of interleukin-12 and tumour necrosis factor-alpha release from macrophages. *Br. J. Pharmacol.* **129**:909-914 (2000).

9.Hasko,G., Szabo,C., Nemeth,Z.H., Kvetan,V., Pastores,S.M. & Vizi,E.S. Adenosine receptor agonists differentially regulate IL-10, TNF-alpha, and nitric oxide production in RAW 264.7 macrophages and in endotoxemic mice. *J. Immunol.* **157**:4634-4640 (1996).

10. Le,M.O *et al.* Adenosine enhances IL-10 secretion by human monocytes. *J. Immunol.* **156**:4408-4414 (1996).

11. Hirschhorn,R., Vawter,G.F., Kirkpatrick,J.A., Jr. & Rosen,F.S. Adenosine deaminase deficiency: frequency and comparative pathology in autosomally recessive severe combined immunodeficiency. *Clin. Immunol. Immunopathol.* **14**:107-120 (1979).

12. Ohta,A. *et al.* A2A adenosine receptor protects tumors from antitumor T cells. *Proc. Natl. Acad. Sci. U. S. A* **103**:13132-13137 (2006).

13. Stagg,J. *et al.* Anti-CD73 antibody therapy inhibits breast tumor growth and metastasis. *Proc. Natl. Acad. Sci. U. S. A* **107**:1547-1552 (2010).

14. Terp,M.G. *et al.* Anti-human CD73 monoclonal antibody inhibits metastasis formation in human breast cancer by inducing clustering and internalization of CD73 expressed on the surface of cancer cells. *J. Immunol.* **191**:4165-4173 (2013).

15. Zhang,B. CD73 promotes tumor growth and metastasis. *Oncoimmunology.* **1**:67-70 (2012).

16. Allard,B., Pommey,S., Smyth,M.J. & Stagg,J. Targeting CD73 enhances the antitumor activity of anti-PD-1 and anti-CTLA-4 mAbs. *Clin. Cancer Res.* **19**:5626-5635 (2013).

17. Iannone,R., Miele,L., Maiolino,P., Pinto,A. & Morello,S. Adenosine limits the therapeutic effectiveness of anti-CTLA4 mAb in a mouse melanoma model. *Am. J. Cancer Res.* **4**:172-181 (2014).

18. Gobert,M. *et al.* Regulatory T cells recruited through CCL22/CCR4 are selectively activated in lymphoid infiltrates surrounding primary breast tumors and lead to an adverse clinical outcome. *Cancer Res.* **69**:2000-2009 (2009).

19. Curiel,T.J. *et al.* Specific recruitment of regulatory T cells in ovarian carcinoma fosters immune privilege and predicts reduced survival. *Nat. Med.* **10**:942-949 (2004).

20. Alam,M.S. *et al.* CD73 is expressed by human regulatory T helper cells and suppresses proinflammatory cytokine production and Helicobacter felis-induced gastritis in mice. *J. Infect. Dis.* **199**:494-504 (2009).

21. Mandapathil,M. *et al.* Adenosine and prostaglandin E2 cooperate in the suppression of immune responses mediated by adaptive regulatory T cells. *J. Biol. Chem.* **285**:27571-27580 (2010).

22. Dwyer,K.M. *et al.* Expression of CD39 by human peripheral blood CD4+ CD25+ T cells denotes a regulatory memory phenotype. *Am. J. Transplant.* **10**:2410-2420 (2010).

23. Schuler,P.J. *et al.* Phenotypic and functional characteristics of ATP-hydrolysing CD4(+) $CD39^{+}$ $FOXP3^{+}$ and $CD4^{+}$ $CD39^{+}$ $FOXP3^{neg}$ T-cell subsets in patients with cancer. *Eur. J. Immunol.* **42**:1876-1885 (2012).

24. Doherty,G.A. *et al.* CD73 is a phenotypic marker of effector memory Th17 cells in inflammatory bowel disease. *Eur. J. Immunol.* **42**:3062-3072 (2012).

25. Lee,Y. *et al.* Induction and molecular signature of pathogenic TH17 cells. *Nat. Immunol.* **13**:991-999 (2012).

26. Duhen,T. & Campbell,D.J. IL-1beta promotes the differentiation of polyfunctional human $CCR6^{+}CXCR3^{+}$ Th1/17 cells that are specific for pathogenic and commensal microbes. *J. Immunol.* **193**:120-129 (2014).

27. Ramesh,R. *et al.* Pro-inflammatory human Th17 cells selectively express P-glycoprotein and are refractory to glucocorticoids. *J. Exp. Med.* **211**:89-104 (2014).

28. Muranski,P. *et al.* Tumor-specific Th17-polarized cells eradicate large established melanoma. *Blood* **112**:362-373 (2008).

29. Dubin,P.J. & Kolls,J.K. Th17 cytokines and mucosal immunity. *Immunol. Rev.* **226**:160-171 (2008).

30. Machon,C. *et al.* Use of designed experiments for the improvement of pre-analytical workflow for the quantification of intracellular nucleotides in cultured cell lines. *J. Chromatogr. A* **1405**:116-125 (2015).

31. Baecher-Allan,C., Brown,J.A., Freeman,G.J. & Hafler,D.A. CD4+CD25high regulatory cells in human peripheral blood. *J. Immunol.* **167**:1245-1253 (2001).

32. Zielinski,C.E. *et al*. Pathogen-induced human TH17 cells produce IFN-gamma or IL-10 and are regulated by IL-1beta. *Nature* **484**:514-518 (2012).

33. Korn,T., Bettelli,E., Oukka,M. & Kuchroo,V.K. IL-17 and Th17 Cells. *Annu. Rev. Immunol.* **27**:485-517 (2009).

34. Viaud,S. *et al*. Gut microbiome and anticancer immune response: really hot Sh*t! *Cell Death. Differ.* **22**:199-214 (2015).

35. Benevides,L., Cardoso,C.R., Tiezzi,D.G., Marana,H.R., Andrade,J.M. & Silva,J.S. Enrichment of regulatory T cells in invasive breast tumor correlates with the upregulation of IL-17A expression and invasiveness of the tumor. *Eur. J. Immunol.* **43**:1518-1528 (2013).

36. Chen,W.C., Lai,Y.H., Chen,H.Y., Guo,H.R., Su,I.J. & Chen,H.H. Interleukin-17-producing cell infiltration in the breast cancer tumour microenvironment is a poor prognostic factor. *Histopathology* **63**:225-233 (2013).

37. Benevides,L. *et al.* IL17 Promotes Mammary Tumor Progression by Changing the Behavior of Tumor Cells and Eliciting Tumorigenic Neutrophils Recruitment. *Cancer Res.* **75**:3788-3799 (2015).

38. Lan,C., Huang,X., Lin,S., Huang,H., Cai,Q., Lu,J. & Liu,J. High density of IL-17-producing cells is associated with improved prognosis for advanced epithelial ovarian cancer. *Cell Tissue Res.* **352**:351-359 (2013).

39. Kryczek,I. *et al.* Phenotype, distribution, generation, and functional and clinical relevance of Th17 cells in the human tumor environments. *Blood* **114**:1141-1149 (2009).

40. King,A.E., Ackley,M.A., Cass,C.E., Young,J.D. & Baldwin,S.A. Nucleoside transporters: from scavengers to novel therapeutic targets. *Trends Pharmacol. Sci.* **27**:416-425 (2006).

41. Blay,J., White,T.D. & Hoskin,D.W. The extracellular fluid of solid carcinomas contains immunosuppressive concentrations of adenosine. *Cancer Res.* **57**:2602-2605 (1997).

42. Kansas,G.S., Wood,G.S. & Tedder,T.F. Expression, distribution, and biochemistry of human CD39. Role in activation-associated homotypic adhesion of lymphocytes. *J. Immunol.* **146**:2235-2244 (1991).

43. MacKenzie,W.M., Hoskin,D.W. & Blay,J. Adenosine suppresses alpha(4)beta(7) integrin-mediated adhesion of T lymphocytes to colon adenocarcinoma cells. *Exp. Cell Res.* **276**:90-100 (2002).

44. Geoghegan,J.C. *et al.* Inhibition of CD73 AMP hydrolysis by a therapeutic antibody with a dual, non-competitive mechanism of action. *MAbs.* **8**:454-467 (2016).

45. Giraudon-Paoli,M. *et al.* Discovery and characterization of new original blocking antibodies targeting the CD73 immune checkpoint for cancer immunotherapy . *AACR Proceedings* Abstr #2344 (2016).

46. Verronese,E. *et al.* Immune cell dysfunctions in breast cancer patients detected through whole blood multi-parametric flow cytometry assay. *Oncoimmunology.* **5**:e1100791 (2016).

47. Dimeloe,S. *et al.* Human regulatory T cells lack the cyclophosphamide-extruding transporter ABCB1 and are more susceptible to cyclophosphamide-induced apoptosis. *Eur. J. Immunol.* **44**:3614-3620 (2014).

Figures legends

Figure 1: CD39 and CD73 are expressed on distinct subsets of memory CD4$^+$ T cells. (**A**) Representative expression of CD39 and CD73 on CD4$^+$ T cell subsets from HD-blood analyzed by FC. (**B, C, E**) Cumulative data from seventeen donors of the different subsets defined by the expression of CD39 and CD73 among naive CD4$^+$ T cells (B) CD4$^+$ Tregs (C) and CD4$^+$ Teffs (E) (statistical analysis: Friedman Test). (**D**) Tregs were analyzed for CD73 expression by Western Blot analysis (CD73: 70 kDa). (**F**) Intensity of CD73 staining on naive CD4$^+$ T cells and CD4$^+$ Teffs (statistical analysis: Wilcoxon Test).

Figure 2: CD73$^+$CD4$^+$ Teffs are enriched in poly-functional Th1.17 cells. (A) HD-blood CD73$^+$ and CD73^{neg} CD4$^+$ Teffs were analyzed by FC for their composition in T helper subsets. Data represented mean of seven donors **(B)** Transcriptomic analysis was performed on resting or short term activated CD73$^+$ or CD73^{neg} CD4$^+$ Teffs (n = 6), (p-value < 0.05 for the genes presented) and genes related to Th profiles were extracted. **(C)** Percentage of IL-2 or TNF-α, IFN-γ, IL-22, IL-17A producing cells and IFN-γ/IL-17A co-producing cells was assessed by FC on CD73$^+$ (black) and CD73^{neg} (white) CD4$^+$ Teffs from HD-blood after short-term PMA/ionomycin reactivation (statistical analysis: Wilcoxon Test). **(D)** Quantification of cytokines produced by purified HD-blood CD73$^+$ (black) and CD73^{neg} (white) CD4$^+$ Teffs activated for 24h with PMA/ionomycin (n=16 for IL-2,TNFα, IFNγ,IL17A, IL10, IL13, and IL21

with exception due to out of range quantification, and n=10 for IL-22, GM-CSF and IL-3) (statistical analysis: Wilcoxon test). **(E)** MDR1 expression and MDR1 functionality was assessed by FC on $CD73^+$ (black) and $CD73^{neg}$ $CD4^+$ (white) Teffs (statistical analysis: Wilcoxon Test). **(F)** $CD73^+CD4^+$ Teffs frequency in HD-blood and healthy colonic tissues (statistical analysis: Mann-Whitney Test).

Figure 3: $CD73^+$ $CD4^+$ Teffs cooperate with Tregs to degrade ATP into Ado. (**A**) The capacity of HD $CD73^+$ or $CD73^{neg}$ $CD4^+$ Teffs to degrade AMP into Ado, was analyzed after a 2-hour incubation with the stable $AMP_{13C,15N}$ isotope (37.5 µM). Residual and generated metabolites were quantified by mass spectrometry coupled-HLPC and the role of CD73 was confirmed by pre-incubation of cells with the CD73 inhibitor (APCP, 50 µM) for 30 minutes before AMP addition. Experiments were performed in duplicate (n = 3 donors) (statistical analysis: Friedman Test). **(B)** The capacity of HD-blood Tregs alone or co-cultured with $CD73^+$ or $CD73^{neg}$ $CD4^+$ Teffs (ratio 1:1) to degrade ATP into Ado were analyzed after 2 hours' incubation with $ATP_{13C,15N}$ isotope (37.5 µM), residual and generated metabolites were quantified by mass spectrometry coupled-HLPC. The role of CD39 and CD73 were confirmed by pre-incubation of cells with the CD39 inhibitor (ARL-67156, 250 µM) and/or the CD73 inhibitor (APCP, 50 µM) for 30 minutes before ATP addition. Experiments were performed in duplicate (n = 3 donors) (statistical analysis: Friedman Test). **(C)** Cell-sorted $CD39^{neg}$ and $CD39^+$ Treg capacity to degrade $ATP_{13C,15N}$ isotope (37.5 µM) was analyzed by the quantification by mass spectrometry coupled-HLPC of ATP and metabolite (AMP) generated. The role of CD39 was confirmed by pre-incubation of cells with the CD39 inhibitor (ARL-67156, 250 µM). Experiments were performed on 3 donors.

Figure 4: Ado suppresses proliferation and restricts polyfunctional $CD73^+CD4^+$ Teffs to IL-17A secretion. (A) Gene expression profiles of ADA and Ado receptors (AdoRa2a, AdoRa2b) were extracted from transcriptomic analyses of purified resting $CD73^+$ or $CD73^{neg}$ $CD4^+$ Teffs (statistical analysis: two-way ANOVA). **(B)** AdoRa2b and ADA proteins levels in $CD73^+$ and $CD73^{neg}$ $CD4^+$ Teffs before and after 1 or 4 days activation with Expand beads were quantified by Western blot. **(C)** The impact of Ado (75 µM/day) on the proliferation of purified $CD73^+$ or $CD73^{neg}$ $CD4^+$ Teffs after activation using Expand beads (1:4), was assessed by microscopy after 4 days. In some conditions cells were pre-incubated for 30 minutes with

rhADA (1 µg/ml), before adding Ado. Data are representative of three donors. **(D)** The impact of metronomic doses of Ado (37.5 µM or 75 µM/day) on cytokine secretion (IL22, IL-17A, IFN-g, GM-CSF, IL-10, IL-13, IL-21, IL-3) by purified $CD73^+CD4^+$ Teffs was quantified by Multiplex Luminex assay in the supernatant of cells after a 48h-culture period with Expand beads (1:4) (statistical analysis: Friedman Test).

Figure 5: Isolated $CD73^+$ $CD4^+$ Teffs are preferential target of $CD39^+$ Tregs through the generation of Ado. (A-B) The impact of ATP (18.75 µM/day) on **(A)** the proliferation of purified $CD73^+$ or $CD73^{neg}$ $CD4^+$ Teffs alone, or in co-culture with total Tregs (**A**) or cell sorted $CD39^+$ and $CD39^{neg}$ Tregs (**B**) at a ratio of 1:1, was assessed by microscopy **(A)** or by CTV dilution **(B)** 4 days after their activation with Expand beads (ration 1:4). **(C)** Similar experiments were performed using Transwell plates. $CD73^+$ (black) and $CD73^{neg}$ (white) $CD4^+$ Teffs were cultured in the upper and lower chamber, respectively, in the presence of with Expand beads (ratio 1:4), with or without ATP (18,75 µM/day) or Ado (75 µM/day), and total Tregs (R) were added either in the upper or lower chamber. **(D-E)** The impact of ATP was also assessed on the proliferation of $CD73^+$ and $CD73^{neg}$ $CD4^+$ Teffs, after the addition of Tregs, all present at a physiological ratio (20%/70%/10%), by microscopy and by FC, by measuring the dilution of proliferation markers (CTV: $CD73^+CD4^+$ Teffs; CFSE: $CD73^{neg}CD4^+$ Teffs). The impact of CD73 and CD39 was assessed by pre-incubating cells with inhibitors of CD73 (APCP: 50 µM) and CD39 (ARL-67156: 250 µM) for 30 minutes.

Figure 6: Breast and ovarian tumors contain highly functional $CD39^+$ Tregs and $CD73^+$ $CD4^+$ Teff with Th1.17 characteristics. (A) Representative FC expression of CD39 and CD73 on Tregs from paired BT and blood sample. **(B)** Representative example of CD39 and CD73 expression on $CD4^+$ Teffs from paired BT and OT and blood samples, by FC. The proportion **(C)** and MFI **(D)** of CD39 expression on Tregs from paired blood and BT (n=11) or OT (n=4) samples were analyzed by FC (statistical analysis: two-way ANOVA). (**E**-**F**) Comparison of CD39% (**E**) and MFI (**F**) of $CD4^+$ Tregs and Teffs within breast (n=11) and ovarian (n=4) tumor environment. (**G**) Purified tumor-infiltrating Tregs were assessed for ATP (37.5 µM) degradation by HPLC, and compared to HD-blood Tregs. Thirty minutes pre-incubation with the CD39 inhibitor (ARL-67156, 250 µM), was used to validate the role of CD39.. **(H)** The proportion $CD73^+CD4^+$ Teffs from paired blood and BT (n=11) or OT (n=4) samples analyzed

by FC (statistical analysis: two-way ANOVA). **(I**) Single cell suspensions of BT (n=12) and OT(n=7) were reactivated with PMA/ionomycin, and single cytokine production (TNF-α, IL-2, IFN-γ and IL-17A) and co-production of IFN-γ and IL-17A were analyzed by FC after gating on $CD73^+$ (black circles) or $CD73^{neg}$ (white circles) Teffs (statistical analysis: two-way ANOVA). (**J**) Localization of Tregs ($FoxP3^+$) and $CD73^+CD4^+$ Teffs was analyzed in frozen human breast tumor section by multi-IF stainings.

Figure 7: $CD73^+$ $CD4^+$ Teffs express less i-ICPs. (A) Representative expression of i-ICPs (TIGIT, CTLA-4, TIM-3, PD-1) and CD73 on $CD4^+$ Teffs from cancer patients blood (Blood-Teff) and paired Tumor-infiltrating $CD4^+$ Teffs (Ti- $CD4^+$ Teff), analyzed by FC. **(B)** Expression of i-ICPs on $CD73^+$ (black) and $CD73^{neg}$ (white) $CD4^+$ Teffs (statistical analysis: Two-way ANOVA) **(C)** Pie chart representing the expression and co-expression of i-ICPs (TIGIT, CTLA-4, TIM-3, PD-1) on $CD73^+$ and $CD73^{neg}$ $CD4^+$ Teffs from BT (n = 10) and OT (n = 10) samples. **(D)** MFI of i-ICPs (CTLA-4, PD-1, TIGIT, TIM-3) expressed on $CD73^{neg}$ versus $CD73^+$ $CD4^+$ Teffs from BT and OT samples (statistical analysis: Two-way ANOVA).

Figure 1

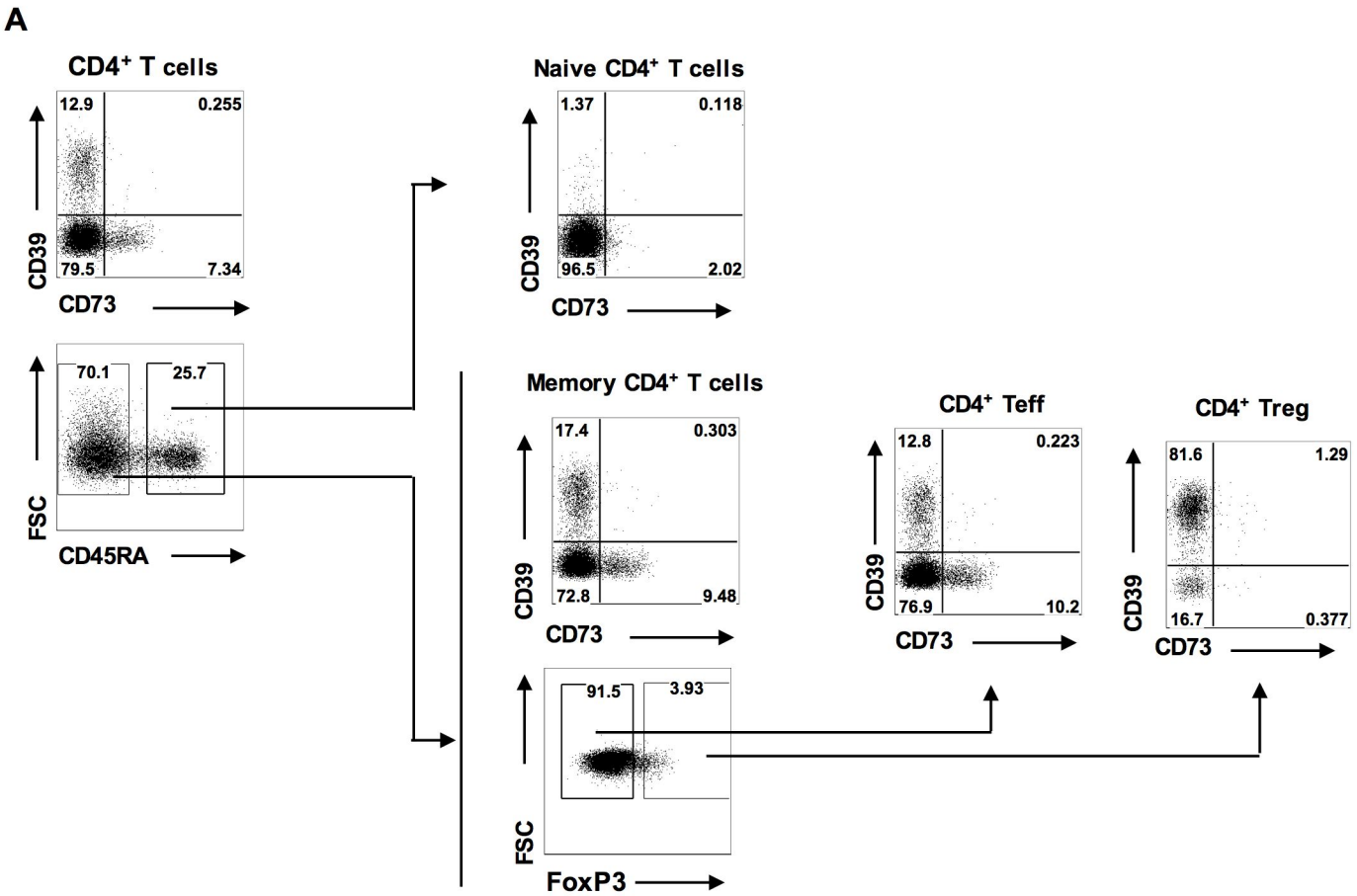

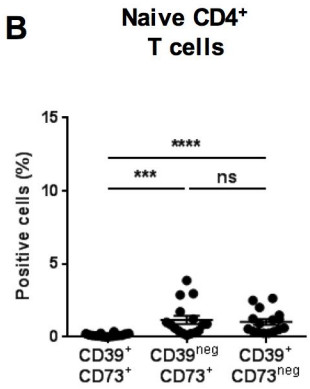

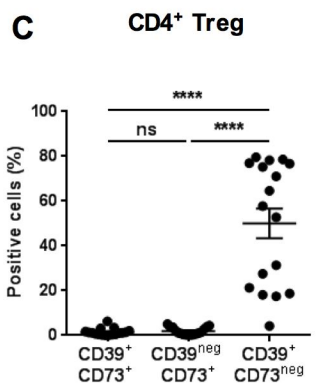

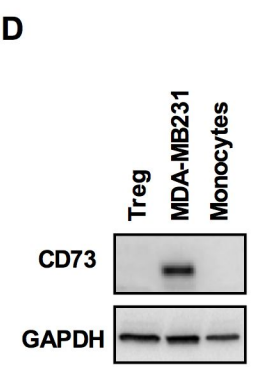

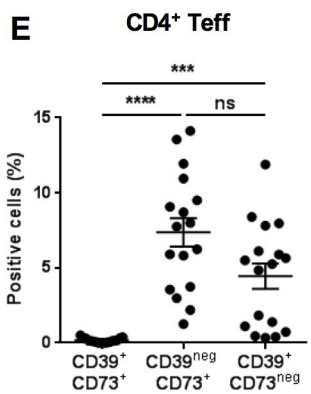

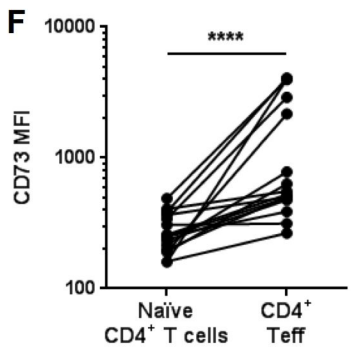

Figure 2

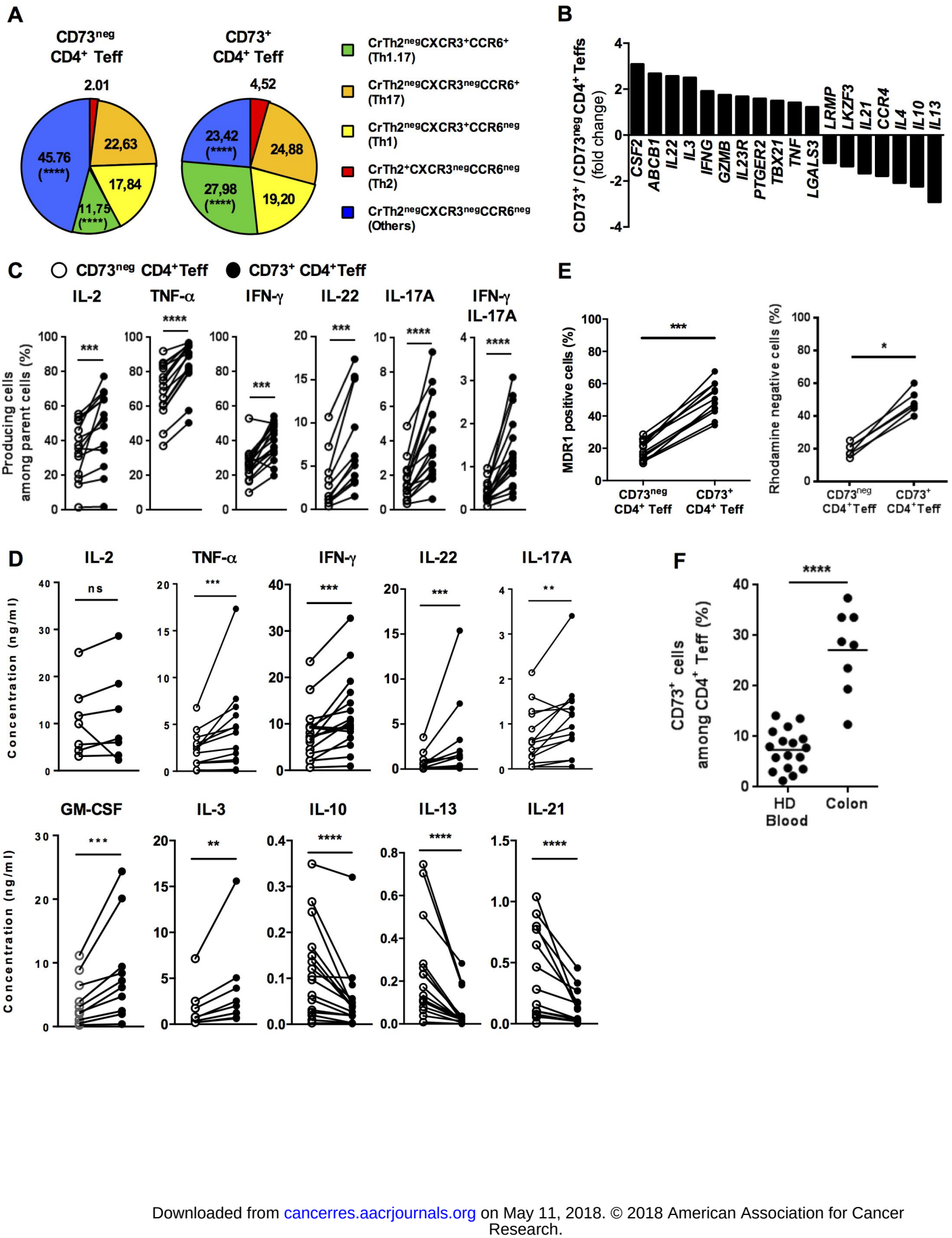

Figure 3

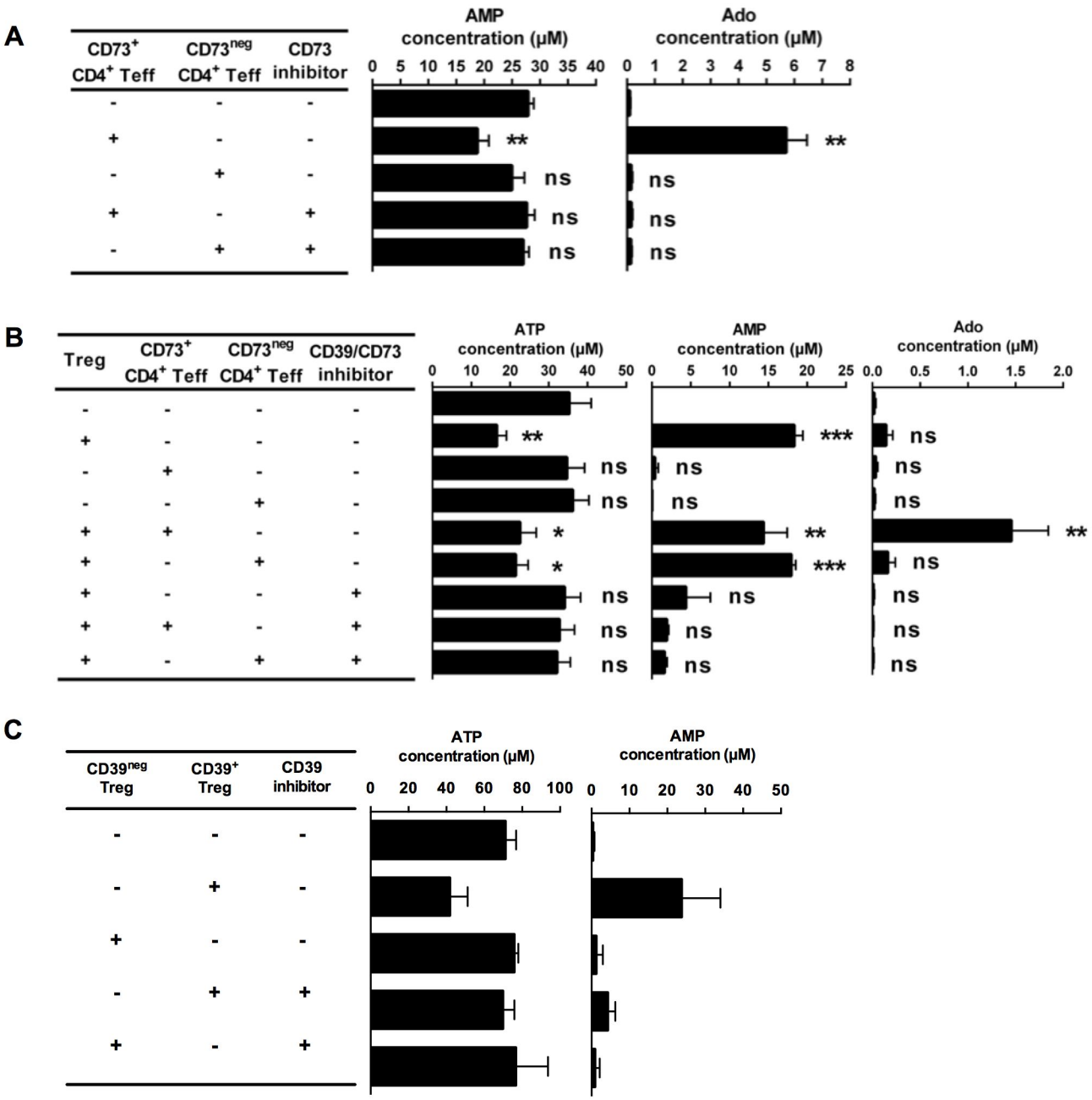

Figure 4

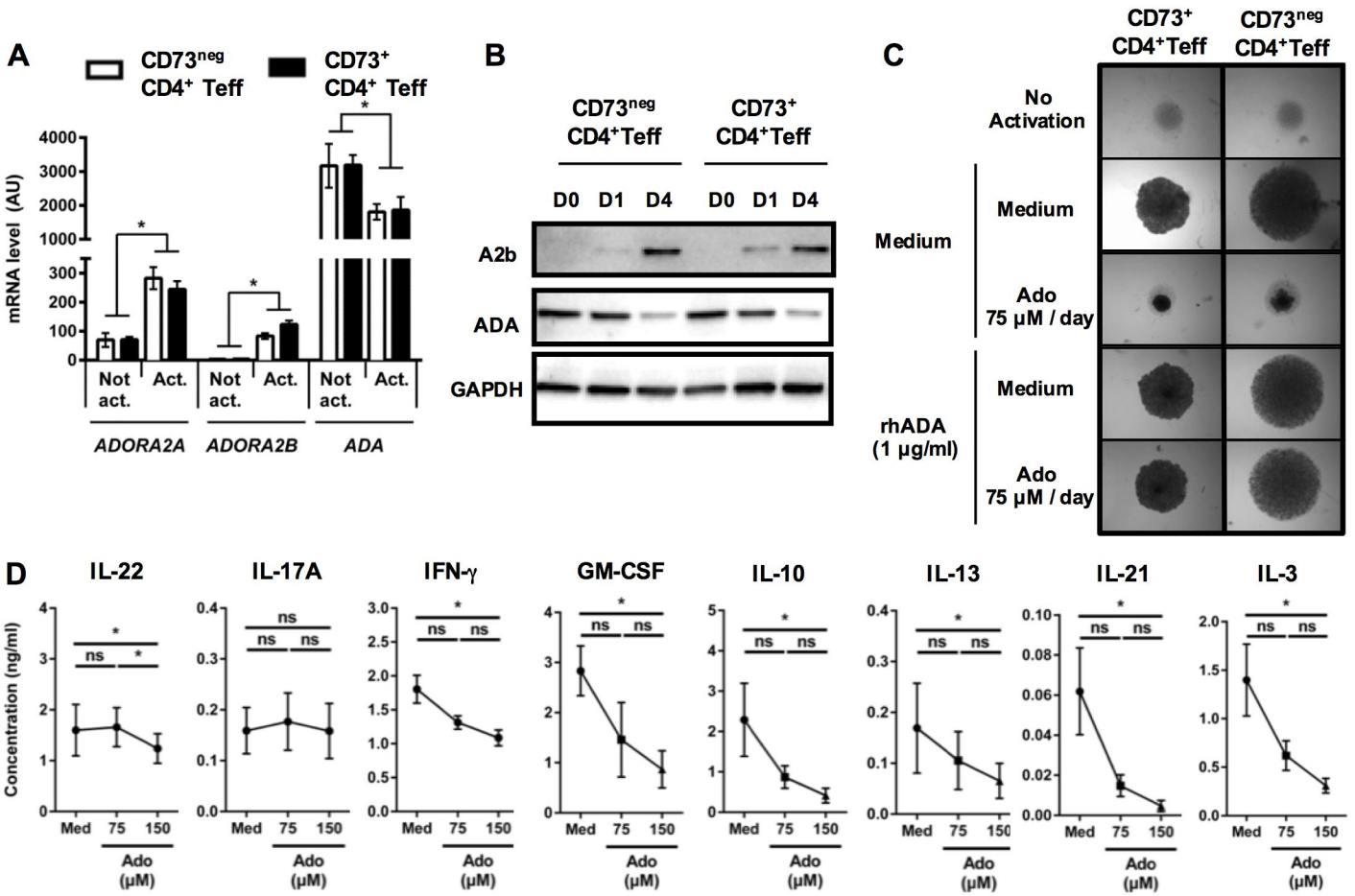

Figure 5

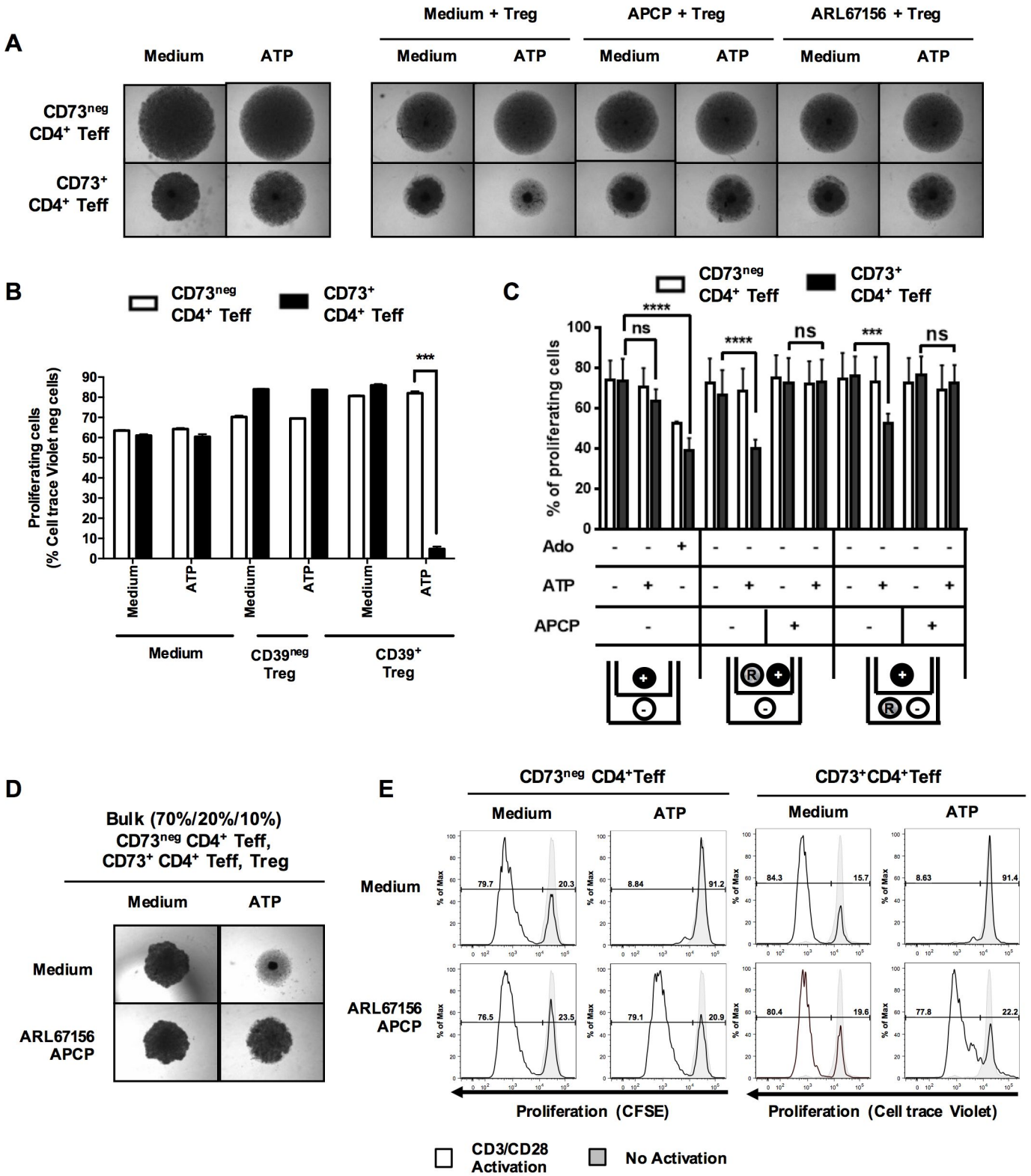

Figure 6

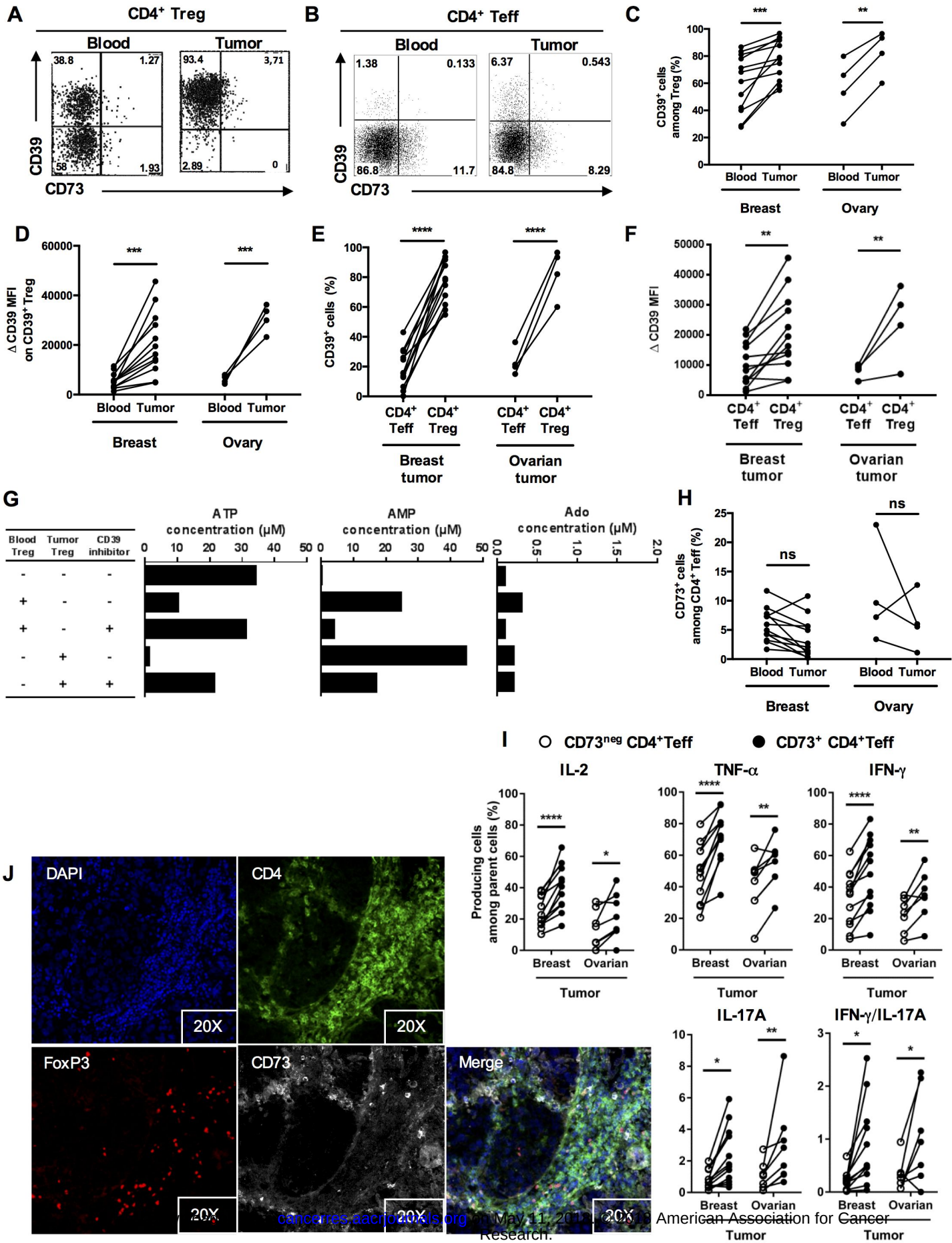

Figure 7

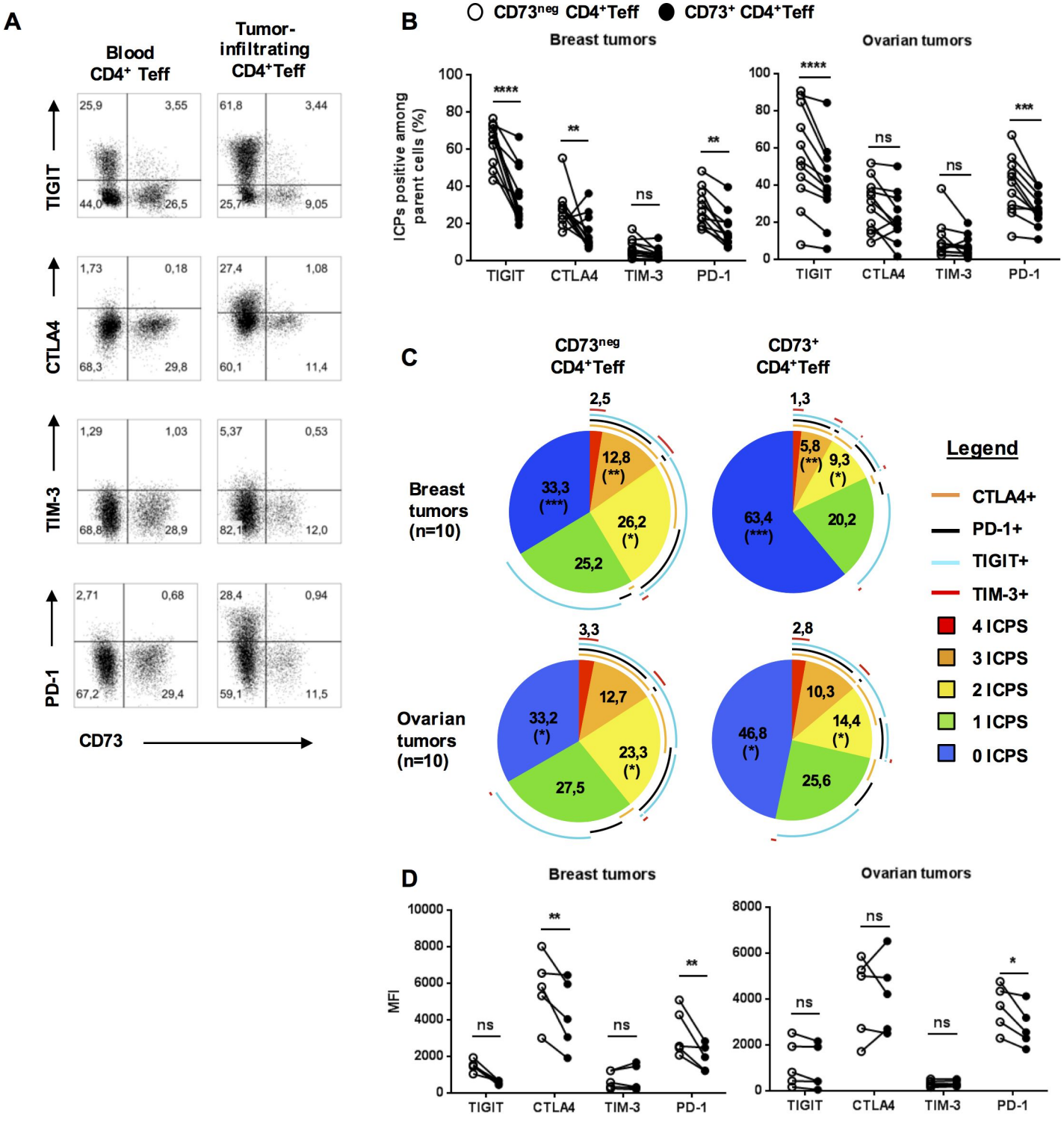

AACR American Association for Cancer Research

Cancer Research

The Journal of Cancer Research (1916–1930) | The American Journal of Cancer (1931–1940)

Autocrine Adenosine regulates tumor polyfunctional CD73+CD4+ effector T cells devoid of immune checkpoints

Nicolas Gourdin, Marion Bossennec, Céline Rodriguez, et al.

Cancer Res Published OnlineFirst March 20, 2018.